Developing a Multivariate Agro-Meteorological Index to Improve Capturing Onset and Persistence of Droughts Utilizing Vapor Pressure Deficit (VPD) and Soil Moisture

Masoud Zeraati [1], Alireza Farahmand [2*], Keyvan Asghari [1], and Ali Behrangi [3]

[1] Department of Civil Engineering, Isfahan University of Technology, Isfahan, Iran.

[2] California State University, Los Angeles.

[3] University of Arizona, Department of Hydrology and Atmospheric Sciences.

*Corresponding author: Alireza Farahmand (afarahm2@calstatela.edu)

Key Points:

- This study introduces a nonparametric agrometeorological drought index by combining vapor pressure deficit and soil moisture information.
- We find this new index detects flash drought and conventional drought onset earlier or at the same time as SPI in evaluated events.
- Results suggest that the proposed index shows drought persistence similar to SSI in assessed events.

Keywords: Drought, Flash Drought, Multivariate Drought Index, VPD, Soil Moisture

Abstract

Drought is associated with adverse environmental and societal impacts across various regions. Therefore, drought monitoring based on a single variable may lead to unreliable information, especially about the onset and persistence of drought. Previous studies show vapor pressure deficit (VPD) data can detect drought onset earlier than other drought indicators such as precipitation. On the other hand, Soil Moisture is a robust indicator for assessing drought persistence. This study introduces a nonparametric multivariate drought index Vapor Pressure Deficit Soil moisture standardized Drought Index (VPDSDI) which is developed by combining vapor pressure deficit (VPD) with soil moisture information. The performance of the multivariate index in terms of drought onset detection is compared with the Standardized Precipitation Index (SPI) for six major drought events across the United States including three flash drought events and three conventional drought events. Additionally, the performance of the proposed index in detecting drought persistence is compared with the Standardized Soil moisture Index (SSI), which is an agricultural drought index. Results indicate the multivariate index detects drought onset always earlier than SPI for conventional events, but VPDSDI detects drought onset earlier than or about the same time as SPI for flash droughts. In terms of persistence, VPDSDI detects persistence almost identical to SSI for both flash and conventional drought events. The results also show that combining VPD with soil moisture reduces the high variability of VPD and produces a smoother index which improves the onset and persistence detection of drought events leveraging VPD and soil moisture information.

Plain Language Summary

Drought has significant negative effects on the environment and society in different areas. Relying on a single variable for drought monitoring can provide unreliable information, particularly when it comes to determining when droughts begin and end. Previous research has found that vapor pressure deficit (VPD) data can identify the beginning of drought conditions earlier than measures like precipitation. In contrast, Soil Moisture has proven to be a reliable indicator for evaluating how long drought conditions last over time. In this study, we introduced a multivariate drought index that combines vapor pressure deficit (VPD) with soil moisture data, named Vapor Pressure Deficit Soil moisture standardized Drought Index (VPDSDI). We compared the performance of this index in detecting drought onset and persistence with SPI and SSI, respectively. The results demonstrate that VPDSDI detects drought onset around the same time or earlier than SPI. Moreover, VPDSDI shows similar detection capabilities to SSI for drought persistence. By combining VPD and soil moisture, VPDSDI reduces variability and provides more reliable information for assessing and understanding drought events.

1 Introduction

Drought is a complex natural hazard that happens at various spatial and temporal scales. Large scale droughts affect several countries simultaneously and result in extensive and severe impacts on food security and may lead to wide-spread famine and fatality within societies (Haile,

2005). The annual economic losses of drought in the United States are estimated by the Federal Emergency Management Agency (FEMA) to be six to eight billion dollars per year (Witt, 1997). Drought early warning and drought onset detection schemes can help decision-makers and water resources managers mitigate the negative impacts of drought on human life and the environment. These planning tools are based on regional drought analysis to quantify the characteristics of drought such as drought onset, duration, intensity, severity, and spatial extent for better improvement of drought monitoring and drought early warning systems (Farahmand et al., 2015; Behrangi et al., 2016; Behrangi et al., 2015).

The mechanism of drought occurrence is complicated, due to the interaction of atmospheric and hydrologic processes. One similarity among most of the drought affected regions is an increase in dry conditions. Drought accompanied by extremely high air temperature and low relative humidity can intensify crop loss and increase wildfire risk (Held et al., 2005). In addition, an increase in air temperature leads to greater evaporation of moisture from soil and vegetation, which eventually increases drought intensity and duration (Held et al., 2005). Besides, changes in ocean temperature and the effects of large-scale annual climatic factors and climate warming on drought formation have become recognized as important factors (Bavar and Kavvas, 1991). Since several factors affect the occurrence of drought, it is difficult to create a comprehensive definition of drought. Conventional drought is generally described as slowly developing, and is categorized into four types: meteorological, agricultural, hydrological, and socioeconomic (wilhite and Glantz, 1985). Meteorological drought is usually characterized as an extended deficit in precipitation; agricultural drought is defined as a deficiency in soil moisture; hydrological drought often occurs when precipitation deficiency over an extended time period affects surface and subsurface water supply; and socioeconomic drought associates the supply and demand of some economic goods with specific elements of meteorological, hydrological, and agricultural drought. A recent study used satellite information to assess drought propagation in the hydrological cycle from meteorological drought to agriculture drought, and finally to hydrological drought (Farahmand et al., 2021).

A new type of drought with rapid onset and intensification, termed “flash drought” has also been recently identified. Flash drought generally begins as a meteorological drought, which eventually leads to an agricultural drought if the conditions continue to exacerbate (Christian et al., 2019). This type of drought is mainly characterized by extremely high air temperature and soil moisture deficit (Mo et al., 2016). Notwithstanding the main cause of drought is a lack of precipitation, but other atmospheric and hydrologic anomalies can also accelerate flash drought development and its severity (Otkin et al., 2018). For instance, low precipitation condition coupled with high evaporative demand as a consequence of high air temperature, low relative humidity, and sunny skies leads to rapidly emerging of agricultural drought condition, mainly known with increasing soil moisture deficits (Otkin et al., 2018). Therefore, several factors can cause a flash drought.

Instead of direct analysis of atmospheric or hydrologic variables, drought indices are often utilized for assessing the drought impacts and analyzing drought characteristics such as onset and termination. Many drought indices, based on different climatic variables (e.g. precipitation, soil moisture, and runoff) have been developed for detecting drought onset, persistence, and termination (Mishra and singh, 2010). These indices have significant differences in terms of strengths and weaknesses in detecting drought onset and termination (Keyantash and Dracup, 2002). One of the most commonly used drought indices for characterizing meteorological drought is the standardized precipitation index (SPI) (Mckee et al., 1993). Several studies found that SPI can detect drought onset earlier than other indices (Shukla et al., 2011; Hayes et al.,1999). On the other hand, (Farahmand et al., 2015) introduced a new drought index based on near surface relative humidity, named standardized relative humidity index (SRHI) that can detect drought onset earlier than SPI. Another novel variable for assessing drought onset is Vapor Pressure Deficit (VPD) which is an atmospheric variable widely used to investigate the impact of surface air temperature on moisture demand of land surface. Recent studies have shown that Standardized Vapor Pressure Deficit Index (SVPDI) can potentially show drought onset earlier than SPI (Behrangi et al., 2015; Behrangi et al., 2016; Farahmand et al., 2023). VPD is calculated by combining air temperature and relative humidity (Gamelin et al., 2022) and measures the difference between the saturated water vapor pressure of the air and the actual amount of water vapor pressure existing in the air. An increase in VPD results in higher water demand in the atmosphere. During wet conditions when precipitation and air moisture are high, VPD is low. On the contrary, during dry conditions when VPD is high, solar radiation heats the surface air temperature as well as soil temperature rather than evaporating water through evapotranspiration, leading to more severe drought (Mankin et al., 2021). Therefore, enhanced VPD is an atmospheric variable that can be a driver of drought and also a consequence of drought (Mankin et al., 2021).

Monitoring drought based on one variable or indicator may not be sufficient because drought has various phases and is hence dependent on multiple hydrologic variables (Hao and Aghakouchak, 2014). For example, meteorological drought, which is generally defined as a precipitation deficit, may develop faster than other types of drought but agricultural drought (deficit in soil moisture) shows the persistence of drought more accurately than meteorological drought (Entekhabi et al., 1996). Recent studies have focused on the development of multivariate drought indices for sufficient and reliable quantification of joint behaviors of hydrologic and climatic variables (Rajsekhar et al., 2014; Kao and Govindaraju, 2010). Multivariate drought indices have shown superior results relative to univariate indices in terms of capturing the early onset and persistence of drought over time (Rad et al., 2017). Therefore, integration of drought information based on indices from various atmospheric and hydrologic sources is necessary for reliable drought characterization in terms of drought onset, persistence, and termination and generally investigating drought structure (Huang et al., 2015).

Several multivariate drought indices based on different combinations of drought-related variables have been developed. For example, the multivariate standardized drought index (MSDI)

(Hao and Aghakouchak, 2013; Hao and Aghakouchak, 2014) probabilistically combines precipitation and soil moisture to investigate drought characteristics including drought onset, persistence, and spatial extent. MSDI has been shown to detect drought onset like SPI and drought persistence similar to Standardized Soil Moisture Index (SSI). The MSDI is an agrometeorological drought index and uses parametric or nonparametric joint probability distribution of precipitation and soil moisture variables. A parametric MSDI requires accurate parameter estimation and goodness-of-fit tests, but a nonparametric MSDI avoids making assumptions regarding the distribution family and significantly reduces the computational burden. In another study, (Zhang et al., 2018) introduced a nonparametric integrated agrometeorological index (MMSDI) similar to MSDI (Hao and Aghakouchak, 2013), but with the addition of evapotranspiration. The inclusion of evapotranspiration develops more realistic drought indices in terms of drought intensity and drought size compared to MSDI.

In general, we hypothesize that multivariate indices (e.g. MSDI and MMSDI) that have precipitation as their meteorological drought factor may not detect drought onset as early as other atmospheric/hydrologic variables such as relative humidity, vapor pressure deficit, and air temperature. Since previous studies concluded that SVPDI (Standardized Vapor Pressure Deficit Index) as a meteorological index can detect drought onset earlier than precipitation (Behrangi et al., 2015; Behrangi et al., 2016; Farahmand et al., 2021; Farahmand et al., 2023) and SSI as an agricultural index can show the persistence of drought more reliable than meteorological indices (Cook et al., 2007; Hao and Aghakouchak, 2014), we introduce a novel indicator which combines information from VPD and soil moisture in this study. Furthermore, soil moisture, air temperature, and relative humidity are all important factors in detecting flash drought. There is also a strong connection between soil moisture and VPD which makes these two variables important for drought monitoring. For instance, low soil moisture can further cause an increase in atmospheric demand which eventually increases VPD (Gentine et al., 2016). In this study, a nonparametric multivariate drought index Vapor Pressure Deficit Soil moisture standardized Drought Index (VPDSDI) is introduced to investigate both conventional and flash drought detection in the continental United States (CONUS). The VPDSDI combines vapor pressure deficit and soil moisture. This index is derived using the National Aeronautics and Space Administration's (NASA) Modern-Era Retrospective Analysis for Research and Applications (MERRA 2). The performance of this index in terms of drought onset and persistence detection is investigated for three major conventional drought events and also for three flash drought events of CONUS. The results are validated against SPI for drought onset and SSI in terms of drought persistence.

2 Study area

In this study, we selected six case studies in the CONUS, as shown in Fig. 1. Selected case studies are divided into two parts of conventional drought events, and flash drought events. The spatial domains of these events are presented in Fig. 1a, and Fig. 1b, respectively. These events are among the major historical droughts in the United States. Fig. 1a shows Conventional droughts of (i) The 2006 Southeastern Drought: Southeastern U.S. experienced severe drought conditions that affected

crops mainly during the 2006 spring-summer period resulting in multi-billion dollar losses (Manuel, 2008; FEMA, 2008); (ii) The 2011 Texas Drought was unique in terms of intensity. Throughout this drought which lasted almost more than a year with below-normal rainfall, major parts of Texas faced a dry fall and winter which eventually led to $7.62 billion in agricultural losses (Nielsen-Gammon, 2012); (iii) The 2020 western US Drought was accompanied by high temperature and low precipitation level. (Williams et al., 2022) found that this drought was the most extreme drought event in the last 1,200 years. This drought especially affected the American Southwest region. Fig. 1b shows Flash droughts of (i) 2019 Southeast flash drought: This drought developed rapidly. During this event, the affected region experienced abnormally dry to exceptional drought conditions (D0-D3, according to U.S. drought monitor) rising from 25% of the area in early September to 80% by the end of the month (Schubert et al., 2020); (ii) 2017 Northern Plain drought: According to United States Drought Monitor (USDM), almost 83% of the Northern plain area experienced abnormally dry conditions during 2017 Northern plain flash drought. This led to severe impacts on agricultural products by decreasing 25% cropland evapotranspiration and 6% reduction in crop products (He et al., 2019); (iii) The 2012 High Plains drought: This drought event was one of the major agricultural disasters in CONUS since 1988. The majority of the Plains and Midwest had below-normal top soil moisture during the 2012 growing season (Rippey, 2015). Low precipitation in addition to extremely high air temperature, low relative humidity, and high evapotranspiration led this event to develop quickly and cause multi-billion dollar economic losses (Farahmand et al., 2015).

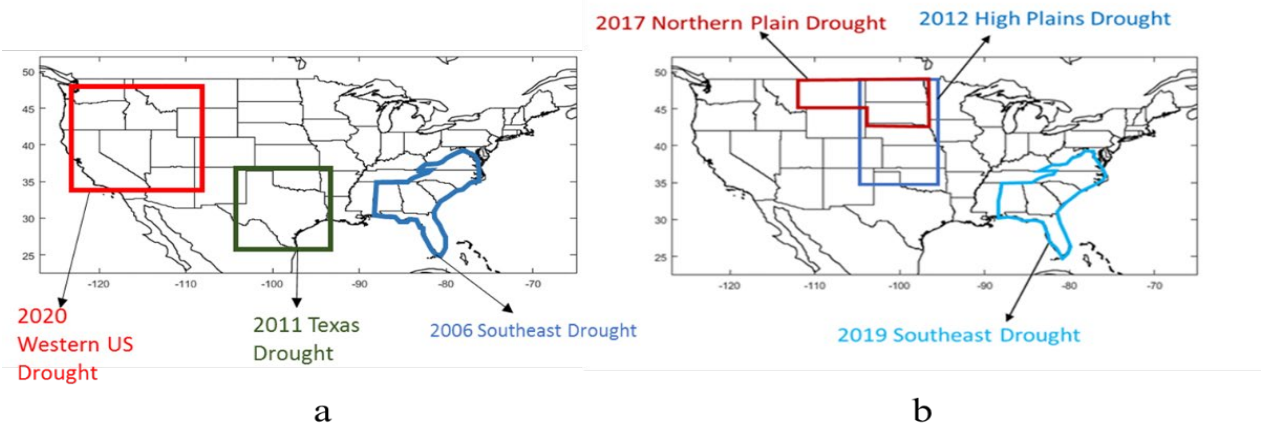

Fig. 1: The location of six major historical drought case studies in the CONUS; (a) conventional drought events, and (b) flash drought events

3 Method and Data

3.1 Datasets

The monthly precipitation (P), soil moisture (SM), and air temperature (T) data were obtained from NASA's second Modern-Era Retrospective analysis for Research and Applications (MERRA2), available at a horizontal resolution of 0.625˚ longitude by 0.5˚ latitude from 1980 onward (Bosilovich, 2015). MERRA2 replaces the MERRA reanalysis (Rienecker et al., 2011) using an upgraded version of the Goddard Earth Observing System Model, Version 5 (GEOS-5) data assimilation. In this study, we used 42 years of data from 1980 to 2022.

Since MERRA2 data does not have surface Relative Humidity (RH) and Vapor pressure deficit (VPD), we have first calculated RH by using T, specific humidity (q), and surface pressure (p). We used Equations S1 to S6 to obtain RH and then calculated VPD using Equations S7 and S8.

3.2 Method

3.2.1 Univariate indices (SPI, SSI, and SVPDI)

Most of the drought indices are derived using a parametric approach. Parametric indices are derived by fitting a parametric function (e.g., normal, gamma, etc.) to data sets. For example, in calculating the original SPI, a two-parameter gamma distribution function is fitted to precipitation records. However, a specific type of distribution function (e.g., gamma) may not fit the entire data. In other words, the gamma distribution function in some cases may not be adequate for describing an observed record of precipitation (Guttman, 1999). Therefore, some studies suggest using location-specific distribution functions or models. However, this leads to statistical inconsistency and incomparability of SPI values (Quiring, 2009; Farahmand and Aghakouchak, 2015). In addition, cross-comparing of drought indices derived by multiple hydrologic variables (e.g., soil moisture or runoff) using the parametric approach also leads to statistical inconsistencies. Farahmand et al. (2015) concluded that non-parametric (empirical) probability functions (e.g., Gringorten) can be used for describing drought information of various hydrologic or atmospheric variables (e.g., precipitation, soil moisture, or relative humidity) in a consistent and comparable scale. The empirical probability function also reduces the computational burden in fitting parametric distribution functions or models. Therefore, in this study, we used a nonparametric approach to compute univariate and multivariate indices. To compute the marginal probability (P) of precipitation, soil moisture, and VPD we used the univariate form of empirical Gringorten plotting position Gringorten (1963):

$$P(x_i) = \frac{i - 0.44}{n + 0.12} \qquad (1)$$

Where $P(x_i)$ is the empirical probability of variable (x), n is the number of the records, and i is the rank of observations from largest to smallest (when used for VPD) or from smallest to largest

(when used for precipitation, or soil moisture). After computing the empirical probability for each variable, the standard index can be expressed as:

$$SI = \emptyset^{-1}(P) \qquad (2)$$

Here, P is the empirical probability computed from equation (1), and $\emptyset$ is standard normal distribution function.

3.2.2 Multivariate Index (VPDSDI)

The proposed VPDSDI is an agrometeorological drought index that combines drought information from vapor pressure deficit and soil moisture. In this study, we used a nonparametric joint distribution function. Empirical joint probability can be calculated using the bivariate form of Gringorten plotting position:

$$P(x_j, y_j) = \frac{m_j - 0.44}{n + 0.12} \qquad (3)$$

Where $P(x_j, y_j)$ is the empirical joint probability of variable (x) and (y), and n is the total number of observations. For the empirical joint probability of pairs of (VPD,SM), m_j is the number of occurrences of (x_i, y_i) satisfying the condition of $x_i \geq x_j$ and $y_i \leq y_j$ $(1 \leq i \leq n)$, which in here x denotes VPD observations and y denotes SM observations. After computing the empirical joint probability of (VPD,SM), the standardized drought index VPDSDI can be computed using equation (2).

3.2.3 Drought threshold and characteristics

The drought threshold was defined according to the classifications of Table 1 (D0 to D4) suggested by Svoboda et al. (2002). We applied the moderate drought threshold (D1) for calculating drought onset (univariate or multivariate index <-0.8). For conventional drought analysis, we used 3-month indices to better understand the slow-evolving changes in variables through time, but for flash drought analysis we used 1-month indices since flash drought develops rapidly and it is important to investigate the occurrence of flash droughts in shorter time scales (Otkin et al., 2018). While previous studies (Christian et al., 2019; Otkin et al., 2018; Mo and Lettenmaier, 2016) have typically utilized shorter time scales (e.g., 5-day) for defining flash droughts, our objective is to assess the potential of this index in capturing flash drought dynamics over an extended temporal period (1-month) similar to approaches taken by (Gamelin et al., 2021; Mcevoy et al., 2016; Noguera et al., 2021). By evaluating the performance of VPDSDI against confirmed flash drought events from previous studies, we aim to demonstrate that if the proposed index effectively detects the flash drought onset and persistence on a 1-month time scale, it could serve as a valuable tool for future studies and enhancing early warning systems. Besides, opting for a 1-month analysis rather than analyzing drought events over a few days allows us to prioritize more severe and prolonged droughts while potentially overlooking shorter-term drought occurrences.

Table1. Drought index classification

Drought type		Range of index
Category	Description	Univariate or multivariate index
D0	Abnormally dry	-0.5 to -0.7
D1	Moderate drought	-0.8 to -1.2
D2	Severe drought	-1.3 to -1.5
D3	Extreme drought	-1.6 to -1.9
D4	Exceptional drought	-2 or less

In order to investigate the characteristics of each drought event, we evaluated five characteristics for each index similar to (Farahmand et al., 2021): the onset month of drought event, the termination month of drought event, drought duration (total number of months between the onset and termination month), maximum drought intensity (minimum value of SI during a drought event), and drought intensity which is expressed as:

$$S = \sum_{i=1}^{D} SI \qquad (4)$$

Where, S is drought intensity, SI is the value of standardized index calculated from equation 2, and D is drought duration.

4 Results and discussion

4.1 Flash Droughts

To illustrate the performance of VPDSDI in detecting flash drought events in terms of onset and persistence, time series of VPDSDI have been compared to SPI, SVPDI, and SSI in three US flash drought events: The 2012 High Plains drought event (Fig. 2a), The 2017 Northern Plains drought event (Fig. 2b) and the 2019 southeast drought event (Fig. 2c). One can see the time series of SVPDI in Fig. 2 for all events to further investigate the effect of VPD as an input in VPDSDI for detecting drought onset. It should be mentioned that for flash drought assessment, we used a 1-month time scale since flash drought events develop rapidly and are sensitive to short term changes in precipitation, soil moisture, relative humidity, and air temperature.

As shown in Fig. 2a, meteorological indices including SVPDI and SPI, show high variability because of the transient nature of these variables and their computation in short periods (1-month). One can see that SPI detects an event that starts in June 2012 and lasts in September 2012. SVPDI

shows a drought event from March 2012 to September 2012. Due to the high variability of SVPDI, we only consider a drought event when an index falls below the threshold continuously. SSI detects a drought event between July 2012 and May 2013. Finally, VPDSDI shows a drought starting from October 2011 to May 2013. VPDSDI detects the onset of this event 8 months earlier than SPI, 5 months earlier than SVPDI, and shows the persistence of this event similar to SSI. As shown in the time series of VPDSDI in Fig. 2a, and by comparing VPDSDI with the time series of SVPDI and SSI, it can be concluded that the agricultural (soil moisture) component of VPDSDI reduces the high variability of meteorological component (VPD) and produces a smoother index which is more reliable for drought persistence detection. Given the comparatively long lead time of VPDSDI compared to other indices studied here, we argue that it is crucial to exercise caution in setting expectations and avoid positioning VPDSDI as a complete substitute for existing indices. Once the early warning signals are detected, we can also consider examining other drought indices in order to mitigate the risk of false drought alarms. However, it is worth noting that VPDSDI possesses unique features that make it a valuable drought index as it combines information from both VPD and soil moisture, recognized as key factors in identifying flash droughts.

Fig. 2b exhibits the time series of the 2017 Northern Plains drought. SPI and SVPDI illustrate a drought event starting in May 2017 to July 2017. As shown, SSI only fell one month below the threshold in July 2017. On the other hand, VPDSDI detects a drought event that starts in May 2017 (similar to SVPDI) and lasts in August 2017, one month later than other indices. The longer drought duration of VPDSDI is due to the slower recovery rate of soil moisture and joint effect of VPD and soil moisture and we argue that this could add more information into the development of this event through the lens of joint occurrence of VPD and soil moisture.

Finally, Fig. 2c shows the time series of the 2019 Southeast drought. It can be seen that SVPDI and SPI indicate a drought event for only one month in September 2019. This event was accompanied by extremely high air temperature, low precipitation, low relative humidity, and high evaporative demand which caused soil moisture to dry quickly. As shown, SSI shows a drought event from September to October 2019, indicating that meteorological and agricultural drought started concurrently. In other words, extreme conditions of the atmosphere depleted soil moisture quickly which led to an agricultural drought. One can see that VPDSDI detects the onset of this event similar to SVPDI, SPI, and SSI in September 2019, but shows the termination of the 2019 Southeast drought like SSI in November 2019. Previous studies also found that during September 2019, dry conditions rose from 25% to 80% at the end of the month in the U.S. Southeast (Schubert et al., 2020). Dry conditions were first initiated by extremely high air temperature and low precipitation which eventually led to low soil moisture conditions. During this event, SVPDI and SPI showed a more intense drought in September 2019 than SSI. The drought intensity of VPDSDI is like its meteorological component (VPD).

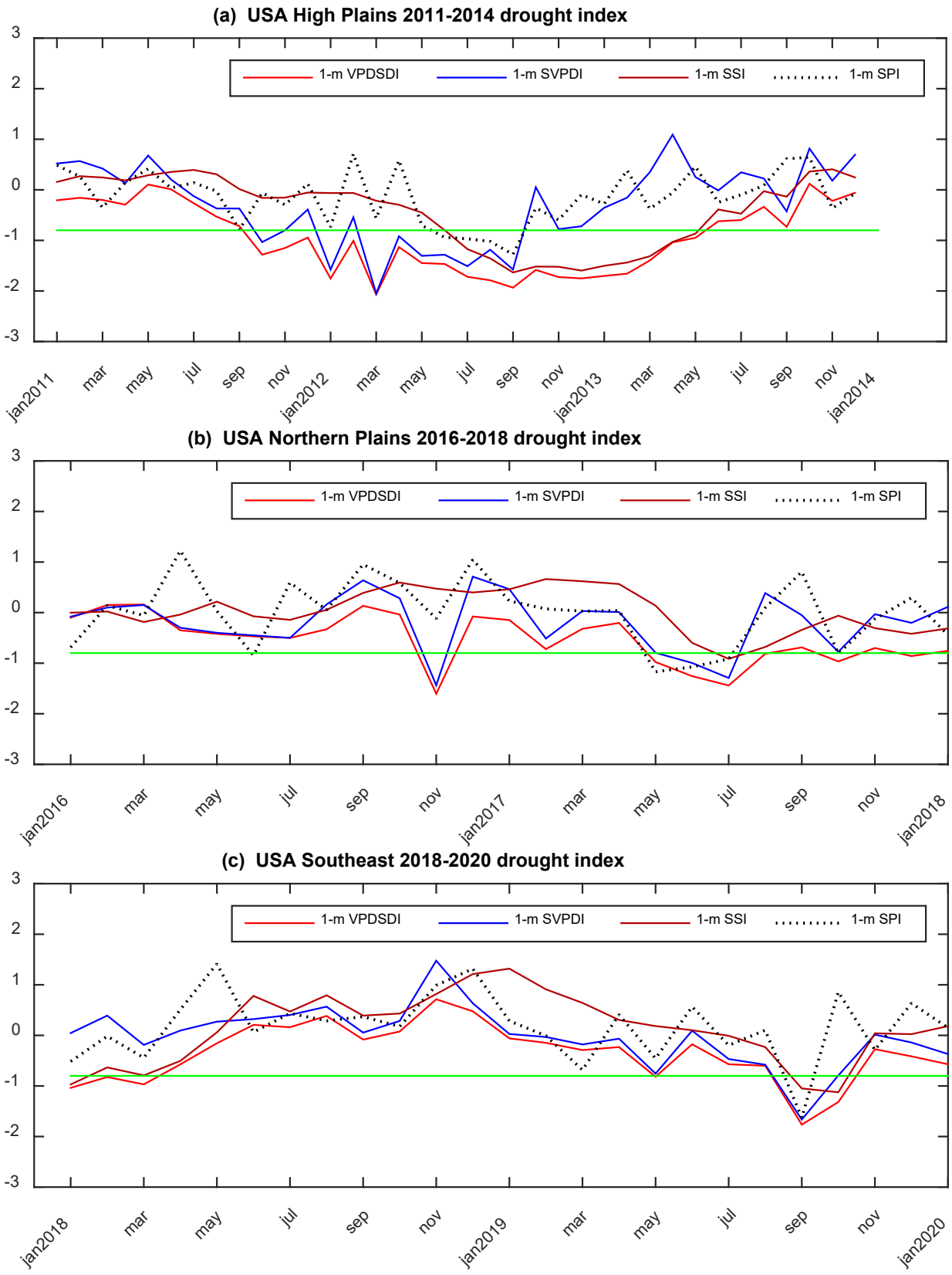

Fig. 2. Time series of 1-month VPDSDI, SVPDI, SPI, and SSI for (a) the 2012 High Plains flash, (b) the 2017 Northern Plains flash drought, and (c) the 2019 Southeast flash drought.

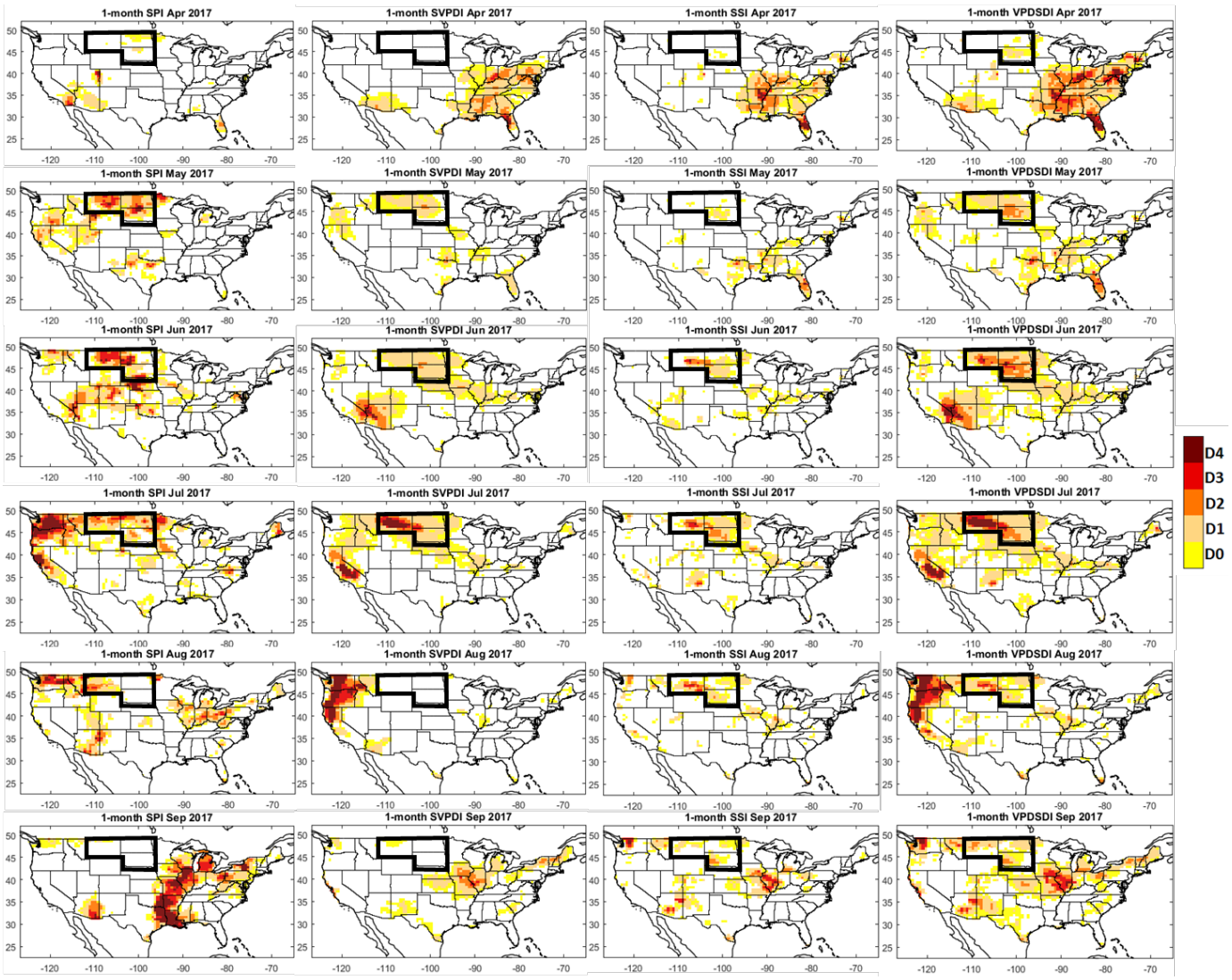

Fig. 3 | (left to right) MERRA2–based 1-month: SPI, SVPDI, SSI, and VPDSDI. (top to bottom) April-September 2017.

To further investigate the spatial development and performance of VPDSDI, SVPDI, SSI, and SPI in detecting flash drought events, maps of 1-month indices for the 2017 Northern Plains drought are presented in Fig. 3. In Fig. 3, the first column shows the 1-month SPI while the second, third, and fourth columns display SVPDI, SSI, and VPDSDI respectively for 2017 Northern Plains drought. These maps provide a visual representation of how each index captures and represents the intensity of drought conditions during that period based on drought intensity categories presented in Table 1 (Svoboda et al., 2002). For further analysis on the spatial development of other flash drought events including the 2012 High Plains drought and the 2019 Southeast drought, readers are directed to Fig. S1 and Fig. S2 respectively. These figures present MERRA2–based 1-month VPDSDI, SVPDI, SSI, and SPI for the 2012 High Plains drought and 2019 Southeast drought, and all maps follow similar patterns discussed in Fig. 3.

As shown in Fig. 3, a few pixels in selected area showed drought condition detected by VPDSDI, SSI, and SPI during April 2017 (first row in Fig. 3). Similar to what discussed in the time series of 2017 Northern Plains event, this drought event started at May 2017 (second row in Fig. 3). In Fig. 3, VPDSDI pattern is consistent with SVPDI during the early stages of the 2017 drought event. While certain areas experienced drought conditions during April 2017, the severity and extent of these conditions were not significant enough to classify the entire region as experiencing moderate drought. One can see that, SSI shows drought conditions in most of the region only in July 2017. Starting in May 2017, extreme and severe drought conditions were observed by SPI, SVPDI, and VPDSDI that were extended until July 2017 while VPDSDI shows drought conditions for one more month in August 2017.

As discussed in the time series of the 2017 Northern Plains flash drought event, the late response of SSI in detecting drought can be attributed to the inherent characteristics of soil moisture, which exhibits a temporal lag in reflecting drought indications when compared to VPD or precipitation patterns. Besides, as we have mentioned in Fig. 2, one of the reasons for the longer drought duration showed by VPDSDI in this event is the joint effect of VPD and soil moisture, which can be seen in maps of September. As shown, VPDSDI accumulates drought signals from VPD (in the northwest of the region) and soil moisture (scattered all over the region), which results in a more severe drought during September all over the region. It should be noted that a previous study (Gerken et al., 2018) showed that some parts of the Northern Plains experienced drought conditions during September 2017 according to Global Historical Climatology Network and USDM. We argue that the inclusion of this aspect can contribute additional insights into the progression of this phenomenon by examining the concurrent existence of VPD and soil moisture. Thus, VPDSDI can present more reliable information about the onset and persistence of this event by combining information from VPD and soil moisture, consistent with previous studies (Gerken et al., 2018; Hoel et al., 2020).

To further illustrate the spatial development of the 2017 Northern Plain drought, Fig. 4 shows the percentage of the region that was under drought conditions from April to September 2017 for SPI, SSI, SVPDI, and VPDSDI. Similarly, Fig S3 and S4 show the proportion of regions that are under drought conditions in the 2012 High Plains and the 2019 Southeast drought event, respectively.

The primary cause of the onset of the 2017 Northern Plain drought was the limited amount of rainfall in May and June, which are typically the wettest months. Additionally, higher-than-normal daytime temperatures also played a role in accelerating the drying process of the land surface (Hoel et al., 2020). As shown in Fig. 4, this event started with a significant decrease in precipitation across a major part of the region as well as an extreme increase in VPD in the vast majority of the region leading to wide-spreading meteorological drought detected by SPI and SVPDI during the early stages of 2017 event in May and June. In the early months of this event, VPDSDI showed drought development similar to SVPDI, and as the drought continued, SPI and SSI showed more than 50 percent of the region under drought conditions in July 2017. Similar to SVPDI and SSI,

the peak of drought affected areas that were detected by VPDSDI occurred in July 2017, with more than 90 percent of the area experiencing drought conditions during this month.

Increased precipitation during the end of July and early August, caused an increase in soil moisture during August, but there was no occurrence of precipitation surpassing the daily average. Furthermore, an exceptional absence of cloudy conditions resulted in a higher influx of solar radiation and unusually elevated daytime maximum temperatures, these climatic factors further contributed to the exacerbation of drought conditions within that period (Hoel et al., 2019). We argue that showing more severe drought by VPDSDI relative to SSI during August and September 2017 could be due to the joint effect of VPD and soil moisture. Soil moisture indicates between 25 and 30 of the region is under drought during August and September according to SSI. Although VPD did not show drought conditions from August to September, a combination of near-normal VPD with below-normal soil moisture has led to a more severe joint effect of VPDSDI. These factors simultaneously affected VPDSDI and led to more severe and wide spread drought than both SVPDI and SSI during August and September.

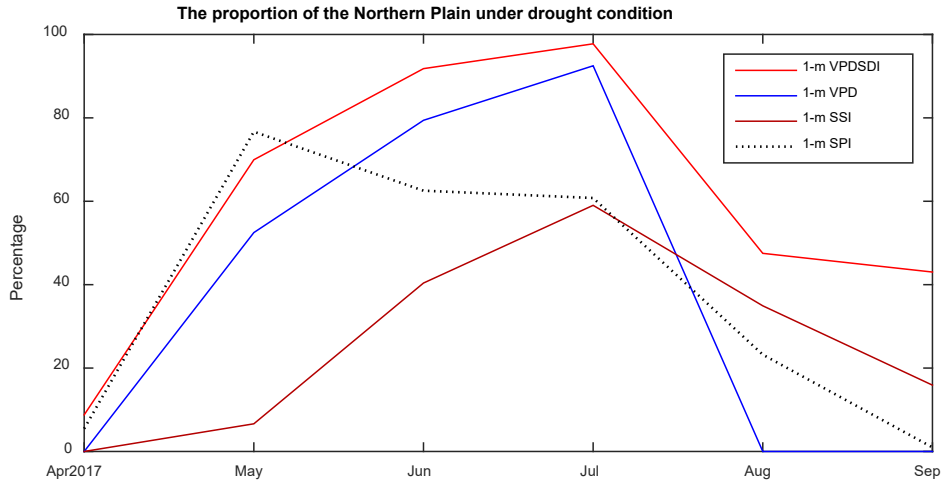

Fig. 4 | Proportion of the Northern Plains that showed drought between April and September 2017

Table 2 presents five important characteristics of each flash drought event including the onset and termination of each index relative to SPI, the minimum value of each index (or maximum intensity of drought), as well as the duration of droughts and drought severity.

As shown in Table 2, for the 2012 High Plains drought, there is a significant difference between drought duration of meteorological indices, SSI, and especially VPDSDI due to the high variability of univariate meteorological indices (SPI and SVPDI). Previous studies also found that the onset of this event was detected by VPD several months before precipitation (Behrangi et al., 2015;

Farahmand et al., 2021). According to Table 2, the 2012 High Plains drought lasted for 20, 11, 7, and 4 months based on VPDSDI, SSI, SVPDI, and SPI, respectively. VPDSDI shows the maximum drought intensity (-2.06), followed by SVPDI (-2.04), SSI (-1.63), and SPI (-1.27). Because of the large duration of VPDSDI and SSI, the drought severity is largest in VPDSDI (-29.5), followed by SSI (-14.94), SVPDI (-9.82), and SPI (-4.2).

As shown in Table 2, the 2017 Northern Plains drought persisted for 4 months according to VPDSDI, lasted 3 months according to SVPDI and SPI, and lasted 1 month according to SSI. Maximum intensity is identified by VPDSDI (-1.44), followed by SVPDI (-1.29), SPI (-1.17), and SSI (-0.91). Finally, the drought severity is largest in VPDSDI (-4.48), followed by SPI (-3.16), SVPDI (-3.08), and SSI (-0.91). It is worth mentioning that considering the largest drought duration detected by VPDSDI, the drought severity of VPDSDI is larger than other indicators.

Finally, as presented in Table 2, the 2019 US Southeast drought lasted for 2 months according to VPDSDI and SSI, and 1 month according to SVPDI and SPI. The drought intensity is largest in VPDSDI (-1.76), followed by SVPDI (-1.66), SPI (-1.62), and SSI (-1.12). Since drought intensity and duration of meteorological indicators (SVPDI and SPI) are almost identical, their drought severity is also similar. The drought severity is largest in VPDSDI (-3.08) followed by SSI (-2.17). Finally, since VPDSDI combines information from two variables, it detects a more severe drought than univariate indices like SVPDI, SSI, and SPI.

As indicated in the summary statistics of Table 2, SVPDI detects drought onset earlier than SPI (1 month on average). Precipitation drought signals come with delay, less intensity, and longer persistence than soil moisture, consistent with previous studies (Farahmand et al., 2021). Since VPDSDI combines information from VPD and Soil Moisture, this index indicates the largest duration and severity compared to all other indices (8.7 months and -12.35 severity). Furthermore, VPDSDI onset detection is on average even earlier than SVPDI (1.7 months earlier on average). This is because VPDSDI detects the onset of the 2012 event with a long 5-month lead time relative to SVPDI. Furthermore, VPDSDI termination is almost identical to SSI termination (6 months vs 5.7 months). Finally, VPDSDI intensity is slightly stronger than SVPDI (-1.75 vs -1.66). Since the mechanisms for the development of flash droughts are different than conventional droughts, the performance of VPDSDI in detecting conventional drought events will be discussed in the next section.

440 Table 2. Characteristics of drought events according to Onset, Termination, Duration, Maximum Intensity, and
441 Severity for each case study and summary statistics of flash drought events

Variables	Onset (month)	Termination (month)	Duration (month)	Maximum Intensity	Severity
		High Plains			
SPI	0	4	4	-1.27	-4.2
VPDSDI	-8	12	20	-2.06	-29.50
SVPDI	-3	4	7	-2.04	-9.82
SSI	1	12	11	-1.63	-14.94
		Northern Plains			
SPI	0	3	3	-1.17	-3.16
VPDSDI	0	4	4	-1.44	-4.48
SVPDI	0	3	3	-1.29	-3.08
SSI	3	3	1	-0.91	-0.91
		South East			
SPI	0	1	1	-1.62	-1.62
VPDSDI	0	2	2	-1.76	-3.08
SVPDI	0	1	1	-1.66	-1.66
SSI	0	2	2	-1.12	-2.17
		Summary			
SPI	0±0	2.7 ± 1.52	2.7 ± 1.52	-1.35 ± 0.23	-3 ± 1.29
VPDSDI	-2.7 ± 4.61	6 ± 5.29	8.7 ± 9.86	-1.75 ± 0.31	-12.35 ± 14.86
SVPDI	-1 ± 1.73	2.7 ± 1.52	3.7 ± 3.05	-1.66 ± 0.37	-4.85 ± 4.35
SSI	1.33 ± 1.52	5.7 ± 5.5	4.7 ± 5.5	-1.22 ± 0.37	-6 ± 7.76

442

443

4.2 Conventional Droughts

Similar to flash droughts, for evaluating the performance of VPDSDI in detecting conventional drought events in terms of onset and persistence, time series of VPDSDI have been compared to SPI, SVPDI, and SSI in three US conventional drought events: The 2006 Southeastern drought event (Fig. 5a), The 2011 Texas drought event (Fig. 5b) and the 2020-2022 western US drought event (Fig. 5c).

As shown in Fig. 5a, SPI shows a drought event occurring between March 2006 and May 2006 (Fig. 5a, SPI falls below the threshold, indicated by the green line from March 2006 to May 2006). It can be seen in Fig. 5a that SSI shows an agricultural drought event from April 2006 to September 2006. In this event, VPDSDI and SVPDI show meteorological drought onset two months earlier than SPI in January 2006. SVPDI, as a meteorological drought index, indicates drought termination in September 2006. VPDSDI, however, shows agricultural drought termination similar to SSI in October 2006.

Fig. 5b shows the time-series of VPDSDI, SVPDI, SPI, and SSI for the 2011 Texas drought. In this event, SPI indicates meteorological drought onset in December 2010 and meteorological drought termination in November 2011 while agricultural drought (based on SSI) starts in January 2011 and terminates in January 2012. VPDSDI detects the drought onset similar to SVPDI (October 2010), which is 2 months earlier than SPI, and shows the termination month of agricultural drought similar to SSI in January 2012.

Finally, Fig. 5c shows the time-series of drought indices for the 2020-2022 drought in the Western US. As shown, SPI detects two drought events, one from September 2020 through November 2020 and one spanning from April 2021 through July 2021. Similar to SPI, SVPDI also detects two events, one from September 2020 to January 2021 and one from April 2021 to September 2021. According to SSI, agricultural drought starts in October 2020 and lasts until September 2021. VPDSDI shows the onset of drought 1 month earlier than SPI and SVPDI in August 2020. Since soil moisture is a component of VPDSDI, this index detects the persistence of drought more reliably than SPI and SVPDI and is similar to SSI. While SPI and SVPDI show two separate drought events, SSI detects one continuous event starting with a one-month delay relative to SPI and SVPDI respectively. This is due to the nature of the soil moisture which shows drought signals with delay and smoother compared to the meteorological variables like precipitation or VPD. VPDSDI, which combines information from both VPD and soil moisture, shows one event continuously from August 2020 to September 2021. The results are consistent with previous studies indicating that soil moisture shows drought persistence more reliable than meteorological indices. Furthermore, combining VPD with soil moisture reduces the high variability of VPD and generates a smoother index. Also, one can see that VPDSDI shows drought onset in August 2020 which none of its corresponding components could show a drought signal and this is due to the joint effect of VPD and soil moisture.

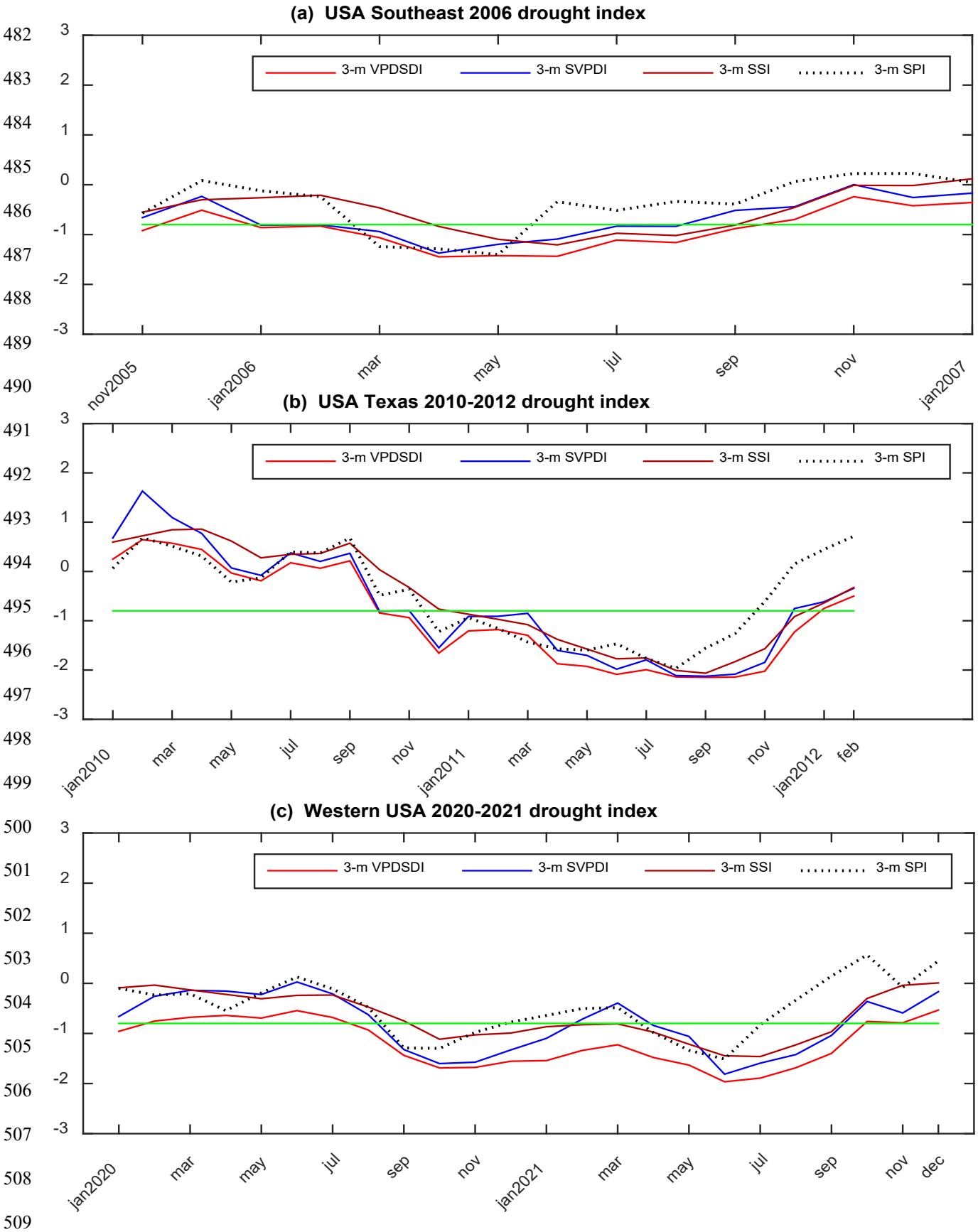

Fig. 5. Time series of 3-month VPDSDI, SVPDI, SPI, and SSI for (a) the 2006 Southeastern drought, (b) the 2011 Texas drought, and (c) the 2020 western US drought.

The spatial maps of VPDSDI, SVPDI, SSI, and SPI are shown for the 2006 Southeastern drought during December 2005-May 2006 period in Fig. 6. The first column shows the 3-month SPI maps, while the second, third, and fourth columns display the 3-month SVPDI, SSI, and VPDSDI maps respectively. To further investigate the spatial development and performance of VPDSDI, SVPDI, SSI, and SPI in detecting other conventional drought events in this study, readers are referred to maps of 3-month indices presented in Figures S5, and S6. Fig. S5 and S6, show MERRA2–based 3-month VPDSDI, SVPDI, SSI, and SPI for the 2011 Texas drought and 2020-2022 Western US drought events respectively.

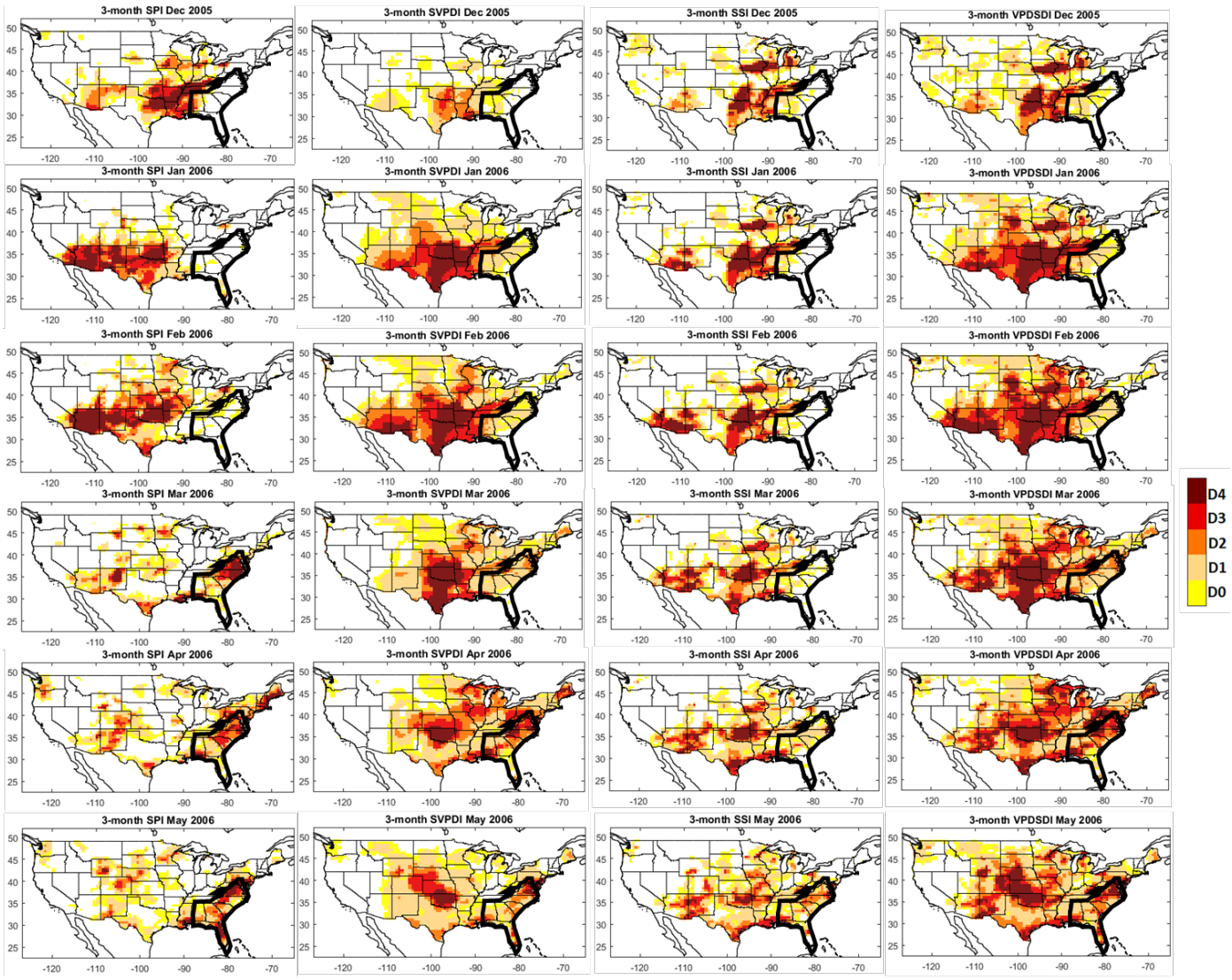

Fig. 6 | (left to right) MERRA2–based 3-month: SPI, SVPDI, SSI, and VPDSDI. (top to bottom) December 2005-May 2006.

From December 2005 to February 2006, SPI and SSI showed moderate and extreme drought conditions across very few parts of the region that were not sufficient to classify the whole region under drought. On the contrary, during January and February 2006, SVPDI and VPDSDI detected extreme and severe drought conditions throughout a vast majority of the southeast, two months earlier than SPI. As drought progresses, SSI shows agricultural drought onset over major parts of the region in April 2006, while one can see that during April, meteorological drought exacerbates and SPI, SVPDI, and VPDSDI show extreme and exceptional drought conditions in some areas during this month. As shown, VPDSDI shows drought onset similar to SVPDI two months earlier than SPI.

Figure 7 presents the 2006 Southeast drought as described by 3-month VPDSDI, SVPDI, SSI, and SPI for the period of June-October 2006. In June 2006, SVPDI, SSI, and VPDSDI showed extreme and severe drought in a large portion of the region. SSI and VPDSDI show the persistence of extreme and severe drought conditions through June to September 2006, while SPI and SVPDI show drought recovery starting from June and August 2006, respectively. Furthermore, VPDSDI is consistent with SSI on the drought persistence, as it shows more severe and expanded drought in the late months of this event which is very similar to SSI indicating an agricultural drought condition. These results illustrate that VPDSDI describes drought onset as early as SVPDI (the meteorological factor) and earlier than SPI while it detects drought persistence similar to SSI (the agricultural component).

To examine the spatial development of the 2006 Southeast drought, Fig. 8 presents the proportion of areas that were under drought condition between December 2005 and October 2006 across the region. To delve deeper into the spatial analysis of VPDSDI, SVPDI, SSI, and SPI in detecting additional conventional drought events examined in this study, we encourage readers to refer to Figures S7 and S8. Fig S7 and S8 illustrate the proportion of the area that was under drought conditions in the 2011 Texas drought and 2020-2022 Western US drought, respectively.

During the early stages of this event, VPDSDI acts similarly to SVPDI in detecting drought affected areas. As shown, there was a major change in drought affected area detected by VPDSDI and SVPDI between December 2005 and January 2006. On the contrary, there were no significant changes in drought detected areas by SPI until February 2006, but SPI suddenly showed a major change in detecting drought areas in March 2006 (two months later than SVPDI and VPDSDI). As drought progresses, agricultural drought detected by SSI starts across the region and more than 50 percent of the US Southeast experienced agricultural drought in April 2006. From April 2006 onward, one can see that although drought detected areas by SVPDI gradually fall, VPDSDI shows under drought areas similar to SSI. These results are consistent with our discussions in the time series of this event and Fig. 7, indicating that VPDSDI shows drought onset similar to SVPDI and also detects agricultural drought termination similar to SSI.

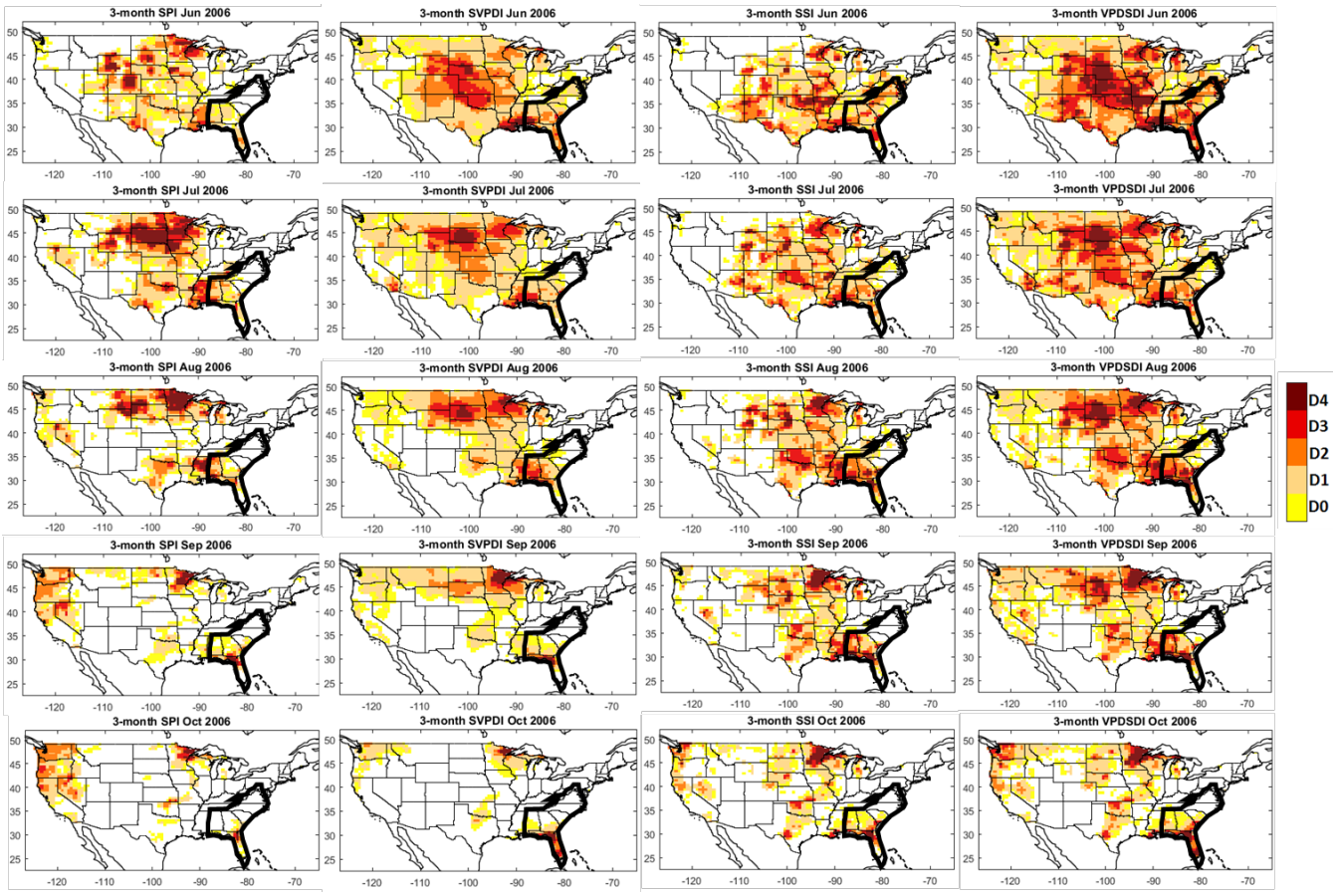

Fig. 7 | (left to right) MERRA2–based 3-month: SPI, SVPDI, SSI, and VPDSDI. (top to bottom) June-October 2006.

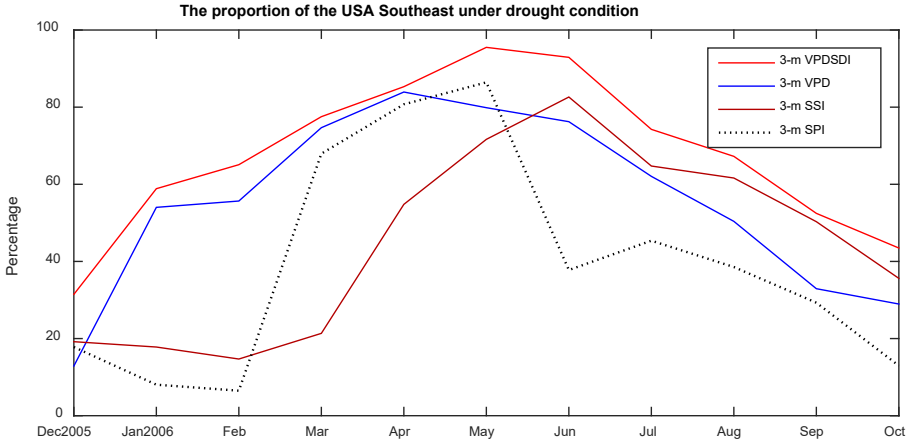

Fig. 8 | Proportion of the USA Southeast that showed drought between December 2005 and October 2006

Table 3 presents five characteristics of each conventional drought event. Similar to Table 2, the characteristics consist of: the onset and termination of each index relative to SPI, minimum value of index for each drought event, duration of droughts, and drought severity.

As shown in Table 3, the 2006 southeast event lasted for 9, 8, 6, and 3 months according to VPDSDI, SVPDI, SSI, and SPI, respectively. VPDSDI and SVPDI detect the onset of this event 2 months earlier than SPI while VPDSDI shows the termination of this event 4 months later than SPI, and concurrently with SSI, indicating the termination of agricultural drought. VPDSDI shows maximum drought intensity of (-1.44), followed by SPI (-1.4), SVPDI (-1.37), and SSI (-1.20). The drought severity is largest in VPDSDI (-10.2), followed by SVPDI (-7.87), SSI (-5.94), and SPI (-3.93).

According to Table 3, in the 2011 Texas event, drought persisted longest in VPDSDI (15 months), followed by SVPDI (14 months), SSI (12 months), and SPI (11 months). The maximum drought intensity is identified by VPDSDI (−2.15), followed by SVPDI (−2.12), SSI (-2.06), and SPI (-1.96). Finally, drought severity is (−24.68), (−21.07), (−17.78), and (−15.93) according to VPDSDI, SVPDI, SSI, and SPI.

Finally, in the 2020-2022 Western U.S. event, drought persisted for 14 months according to VPDSDI, 12 months according to SSI, 11 months according to SVPDI, and 7 months according to SPI. The maximum drought intensity is shown in VPDSDI (−1.96), followed by SVPDI (−1.81), SPI (−1.51), and SSI (-1.46). VPDSDI showed the maximum drought severity (-21.44), SVPDI (-14.69), SSI (-12.92), and SPI (-8.22).

As shown and discussed in Fig. 5 and Table 3, in all conventional drought events, drought onset, and termination signals are transferred with some delay from precipitation to soil moisture, which is consistent with previous studies (Farahmand et al., 2021). Furthermore, results indicated that VPD (SVPDI) detects drought onset earlier than precipitation (SPI). On average, SVPDI detects the onset of droughts 1.33 months earlier than precipitation. Finally, results show that VPDSDI detects conventional drought onset on average 1.66 months earlier than SPI, almost similar to its meteorological component (VPD), and identifies conventional drought persistence similar to its agricultural component soil moisture (11 months). Therefore, VPDSDI duration and severity are the largest compared to all other indices with 12.6 and -18.7 respectively.

602 Table 3. Characteristics of drought events according to Onset, Termination, Duration, Maximum Intensity, and
603 Severity for each case study and summary statistics of conventional drought events

Variables	Onset (month)	Termination (month)	Duration (month)	Maximum Intensity	Severity
		2006 South East			
SPI	0	3	3	-1.40	-3.93
VPDSDI	-2	7	9	-1.44	-10.20
SVPDI	-2	6	8	-1.37	-7.87
SSI	1	7	6	-1.20	-5.94
		2011 Texas			
SPI	0	11	11	-1.96	-15.93
VPDSDI	-2	13	15	-2.15	-24.68
SVPDI	-2	12	14	-2.12	-21.07
SSI	1	13	12	-2.06	-17.78
		2020 Western US			
SPI	0	11	7	-1.51	-8.22
VPDSDI	-1	13	14	-1.96	-21.44
SVPDI	0	13	11	-1.81	-14.69
SSI	1	13	12	-1.46	-12.92
		Summary			
SPI	0±0	8.3±4.6	7±4	-1.6±0.3	-9.3±6.0
VPDSDI	-1.66±0.6	11±3.5	12.6±3.2	-1.85±0.37	-18.7±7.6
SVPDI	-1.33±1.1	10.3±3.8	11±3	-1.76±0.38	-14.5±6.6
SSI	1±0	11±3.5	10±3.5	-1.57±0.44	-12.2±6

604

605

606 ## 5 Conclusions

607 In this study, a new integrated agro-meteorological drought index (VPDSDI) was developed by
608 combining vapor pressure deficit with soil moisture information. 42 years (1980-2022) of data
609 from NASA's Modern-Era Retrospective Analysis for Research and Applications (MERRA 2)
610 product were used for this study. The proposed index was computed by using a multivariate
611 nonparametric approach, which reduces the computational burden. This index was compared to
612 SPI and SSI in terms of timing of drought onset and termination, respectively.

613 Six major historical droughts in the CONUS were selected for analysis. Three flash droughts: the
614 2019 southeast drought, the 2017 Northern Plain drought, and the 2012 High Plains drought; Three
615 conventional drought events: The 2006 Southeastern Drought, the 2011 Texas Drought, and the
616 2020 Western US Drought. Each of the selected drought events has unique characteristics and
617 results show that the newly developed index is capable of detecting drought onset earlier than or
618 at the same time as SPI. Also, this index generally detects agricultural drought termination at the
619 same time as SSI.

620 The comparison of VPDSDI with SPI and SSI for the flash drought events suggests that this index
621 can detect drought onset earlier than or about the same time as SPI with an average of around 2.7
622 months. Besides, VPDSDI shows agricultural drought termination almost the same as SSI. We
623 should note that since flash droughts develop rapidly and are mainly accompanied by high air
624 temperature, low relative humidity, and low soil moisture, univariate indices used in this study
625 including SPI, SVPDI, and SSI may not be able to detect the duration of flash droughts reliably.
626 Since VPDSDI combines information from both VPD and soil moisture, it can potentially detect
627 the rapid onset, intensification, and persistence of flash droughts more reliably than other
628 univariate indices.

629 The comparison of VPDSDI with SPI and SSI for the conventional drought events indicates that
630 VPDSDI captures the onset of this type of drought on average 1.66 months earlier than SPI in all
631 three events. This is due to the skill of the VPD component of VPDSDI as well as the combination
632 of VPD with soil moisture which improves the ability of VPDSDI in detecting drought onset.
633 Furthermore, the results show that VPDSDI captures drought persistence similar to SSI. This
634 behavior is due to the soil moisture information used for deriving VPDSDI.

635 Finally, we showed that combining VPD with soil moisture reduces the high variability of VPD
636 which produces a smoother and more reliable drought index. The new index could add further
637 insight into the development of drought events by looking at the joint distribution of
638 meteorological variables (VPD) and soil moisture. We emphasize that VPDSDI should not replace
639 other drought indicators and can be used as an additional source of information along with other
640 drought indices.

641

Open Research

The data used for this study are freely available for Surface Pressure, Surface Air Temperature, and Specific Humidity :https://disc.gsfc.nasa.gov/datasets/M2IMNXLFO_5.12.4/summary; For precipitation and soil moisture: https://disc.gsfc.nasa.gov/datasets/M2TMNXLND_5.12.4/summary.

References

AghaKouchak, A., and A. Mehran (2013), Extended contingency table: Performance metrics for satellite observations and climate model simulations, *Water Resources Research*, *49*(10), 7144-7149.

Alduchov, O. A., and R. E. Eskridge (1996), Improved Magnus form approximation of saturation vapor pressure, *Journal of Applied Meteorology*, *35*(4), 601-609.

Behrangi, A., E. J. Fetzer, and S. L. Granger (2016), Early detection of drought onset using near surface temperature and humidity observed from space, *International Journal of Remote Sensing*, *37*(16), 3911-3923.

Behrangi, A., P. Loikith, E. Fetzer, H. Nguyen, and S. Granger (2015), Utilizing humidity and temperature data to advance monitoring and prediction of meteorological drought, *Climate*, *3*(4), 999-1017.

Bravar, L., and M. Kavvas (1991), On the physics of droughts. I. A conceptual framework, *Journal of Hydrology*, *129*(1-4), 281-297.

Christian, J. I., J. B. Basara, J. A. Otkin, E. D. Hunt, R. A. Wakefield, P. X. Flanagan, and X. Xiao (2019), A Methodology for Flash Drought Identification: Application of Flash Drought Frequency across the United States, *Journal of Hydrometeorology*, *20*(5), 833-846.

Cook, E. R., R. Seager, M. A. Cane, and D. W. Stahle (2007), North American drought: Reconstructions, causes, and consequences, *Earth-Science Reviews*, *81*(1), 93-134.

Entekhabi, D., I. Rodriguez-Iturbe, and F. Castelli (1996), Mutual interaction of soil moisture state and atmospheric processes, *Journal of Hydrology*, *184*(1-2), 3-17.

Farahmand, A., and A. AghaKouchak (2015), A generalized framework for deriving nonparametric standardized drought indicators, *Advances in Water Resources*, *76*, 140-145.

Farahmand, A., A. AghaKouchak, and J. Teixeira (2015), A vantage from space can detect earlier drought onset: An approach using relative humidity, *Scientific reports*, *5*, 8553.

Farahmand, A., J. T. Reager, and N. Madani (2021), Drought Cascade in the Terrestrial Water Cycle: Evidence From Remote Sensing, *Geophysical Research Letters*, *48*(14), e2021GL093482.

Farahmand, A., S. Ray, H. Thrastarson, S. Licata, S. Granger, and B. Fuchs (2023), A Workshop on Using NASA AIRS Data to Monitor Drought for the U.S. Drought Monitor, *Bulletin of the American Meteorological Society*, *104*(1), E22-E30.

(FEMA), F. E. M. A. (2008), Billion dollar U.S. weather disasters, edited.

675 Gamelin, B. L., J. Feinstein, J. Wang, J. Bessac, E. Yan, and V. R. Kotamarthi (2022), Projected U.S. drought extremes
676 through the twenty-first century with vapor pressure deficit, *Scientific Reports*, *12*(1), 8615.

677 Gentine, P., A. Chhang, A. Rigden, and G. Salvucci (2016), Evaporation estimates using weather station data and
678 boundary layer theory, *Geophysical Research Letters*, *43*(22), 11,661-611,670.

679 Gerken, T., G. T. Bromley, B. L. Ruddell, S. Williams, and P. C. Stoy (2018), Convective suppression before and
680 during the United States Northern Great Plains flash drought of 2017, *Hydrology and Earth System Sciences*, *22*(8),
681 4155-4163.

682 Gringorten, I. I. (1963), A plotting rule for extreme probability paper, *Journal of Geophysical Research*, *68*(3), 813-
683 814.

684 Guttman, N. B. (1999), Accepting the standardized precipitation index: a calculation algorithm 1, *JAWRA Journal of*
685 *the American Water Resources Association*, *35*(2), 311-322.

686 Haile, M. (2005), Weather patterns, food security and humanitarian response in sub-Saharan Africa, *Philosophical*
687 *Transactions of the Royal Society B: Biological Sciences*, *360*(1463), 2169-2182.

688 Hao, Z., and A. AghaKouchak (2013), Multivariate standardized drought index: a parametric multi-index model,
689 *Advances in Water Resources*, *57*, 12-18.

690 Hao, Z., and A. AghaKouchak (2014), A nonparametric multivariate multi-index drought monitoring framework,
691 *Journal of Hydrometeorology*, *15*(1), 89-101.

692 Hayes, M. J., M. D. Svoboda, D. A. Wiihite, and O. V. Vanyarkho (1999), Monitoring the 1996 drought using the
693 standardized precipitation index, *Bulletin of the American meteorological society*, *80*(3), 429-438.

694 He, M., J. S. Kimball, Y. Yi, S. Running, K. Guan, K. Jensco, B. Maxwell, and M. Maneta (2019), Impacts of the
695 2017 flash drought in the US Northern plains informed by satellite-based evapotranspiration and solar-induced
696 fluorescence, *Environmental Research Letters*, *14*(7), 074019.

697 Held, I. M., J. Delworth Tl Fau - Lu, K. L. Lu J Fau - Findell, T. R. Findell Kl Fau - Knutson, and T. R. Knutson
698 (2005), Simulation of Sahel drought in the 20th and 21st centuries(0027-8424 (Print)).

699 Hoell, A., J. Perlwitz, and J. K. Eischeid (2019), The causes, predictability, and historical context of the 2017 US
700 Northern Great Plains drought.

701 Hoell, A., B.-A. Parker, M. Downey, N. Umphlett, K. Jencso, F. A. Akyuz, D. Peck, T. Hadwen, B. Fuchs, and D.
702 Kluck (2020), Lessons learned from the 2017 flash drought across the US Northern Great Plains and Canadian Prairies,
703 *Bulletin of the American Meteorological Society*, 1-46.

704 Kao, S.-C., and R. S. Govindaraju (2010), A copula-based joint deficit index for droughts, *Journal of Hydrology*,
705 *380*(1-2), 121-134.

706 Keyantash, J., and J. A. Dracup (2002), The quantification of drought: an evaluation of drought indices, *Bulletin of*
707 *the American Meteorological Society*, *83*(8), 1167-1180.

708 Koster, R. D., M. G. Bosilovich, S. Akella, C. Lawrence, R. Cullather, C. Draper, R. Gelaro, R. Kovach, Q. Liu, and
709 A. Molod (2015), Technical report series on global modeling and data assimilation, volume 43. MERRA-2; initial
710 evaluation of the climate.

711 Lawrence, M. G. (2005), The relationship between relative humidity and the dewpoint temperature in moist air: A
712 simple conversion and applications, *Bulletin of the American Meteorological Society*, *86*(2), 225-234.

713 Mankin, J. S., I. Simpson, A. Hoell, R. Fu, J. Lisonbee, A. Sheffield, and D. Barrie (2021), NOAA Drought Task
714 Force Report on the 2020–2021 Southwestern U.S. Drought.

715 Manuel, J. (2008), Drought in the Southeast: Lessons for Water Management, *Environmental Health Perspectives*,
716 *116*(4), A168-A171.

717 Maxwell, J., and P. Soule (2009), United States Drought of 2007: Historical Perspectives, *Climate Research*, *38*, 95-
718 104.

719 McEvoy, D. J., J. L. Huntington, M. T. Hobbins, A. Wood, C. Morton, M. Anderson, and C. Hain (2016), The
720 evaporative demand drought index. Part II: CONUS-wide assessment against common drought indicators, *Journal of*
721 *Hydrometeorology*, *17*(6), 1763-1779.

722 McKee, T. B., N. J. Doesken, and J. Kleist (1993), The relationship of drought frequency and duration to time scales,
723 paper presented at Proceedings of the 8th Conference on Applied Climatology, American Meteorological Society
724 Boston, MA.

725 Mishra, A. K., and V. P. Singh (2010), A review of drought concepts, *Journal of hydrology*, *391*(1-2), 202-216.

726 Mo, K. C., and D. P. Lettenmaier (2016), Precipitation Deficit Flash Droughts over the United States, *Journal of*
727 *Hydrometeorology*, *17*(4), 1169-1184.

728 Nielsen-Gammon, J. W. (2012), The 2011 Texas Drought, *Texas Water Journal*, *3*(1), 59-95.

729 Noguera, I., F. Domínguez-Castro, and S. M. Vicente-Serrano (2021), Flash drought response to precipitation and
730 atmospheric evaporative demand in Spain, *Atmosphere*, *12*(2), 165.

731 Otkin, J. A., M. Svoboda, E. D. Hunt, T. W. Ford, M. C. Anderson, C. Hain, and J. B. Basara (2018), Flash Droughts:
732 A Review and Assessment of the Challenges Imposed by Rapid-Onset Droughts in the United States, *Bulletin of the*
733 *American Meteorological Society*, *99*(5), 911-919.

734 Quiring, S. M. (2009), Developing objective operational definitions for monitoring drought, *Journal of Applied*
735 *Meteorology and Climatology*, *48*(6), 1217-1229.

736 Rad, A. M., B. Ghahraman, D. Khalili, Z. Ghahremani, and S. A. Ardakani (2017), Integrated meteorological and
737 hydrological drought model: A management tool for proactive water resources planning of semi-arid regions,
738 *Advances in Water Resources*, *107*, 336-353.

739 Rajsekhar, D., V. P. Singh, and A. K. Mishra (2015), Multivariate drought index: An information theory based
740 approach for integrated drought assessment, *Journal of Hydrology*, *526*, 164-182.

741 Rienecker, M. M., M. J. Suarez, R. Gelaro, R. Todling, J. Bacmeister, E. Liu, M. G. Bosilovich, S. D. Schubert, L.
742 Takacs, and G.-K. Kim (2011), MERRA: NASA's modern-era retrospective analysis for research and applications,
743 *Journal of climate*, *24*(14), 3624-3648.

744 Rippey, B. R. (2015), The U.S. drought of 2012, *Weather and Climate Extremes*, *10*, 57-64.

745 Schubert, S., Y. Chang, A. Deangelis, H. Wang, and R. Koster (2020), On the Development and Demise of the Fall
746 2019 Southeast U. S. Flash Drought: Links to an Extreme Positive IOD, *Journal of Climate*, *34*.

747 Shukla, S., A. C. Steinemann, and D. P. Lettenmaier (2011), Drought monitoring for Washington State: Indicators
748 and applications, *Journal of Hydrometeorology*, *12*(1), 66-83.

749 Svoboda, M., D. LeComte, M. Hayes, R. Heim, K. Gleason, J. Angel, B. Rippey, R. Tinker, M. Palecki, and D.
750 Stooksbury (2002), The drought monitor, *Bulletin of the American Meteorological Society*, *83*(8), 1181-1190.

751 Wallace, J. M., and P. V. Hobbs (2006), *Atmospheric science: an introductory survey*, Elsevier.

752 Weiss, J. L., J. L. Betancourt, and J. T. Overpeck (2012), Climatic limits on foliar growth during major droughts in
753 the southwestern USA, *Journal of Geophysical Research: Biogeosciences*, *117*(G3).

754 Wilhite, D. A., and M. H. Glantz (1985), Understanding: the Drought Phenomenon: The Role of Definitions, *Water*
755 *International*, *10*(3), 111-120.

756 Williams, A. P., B. I. Cook, and J. E. Smerdon (2022), Rapid intensification of the emerging southwestern North
757 American megadrought in 2020–2021, *Nature Climate Change*, *12*(3), 232-234.

758 Witt, J. L. (1997), *National mitigation strategy: partnerships for building safer communities*, Diane Publishing.

759 Yuan, X., and E. F. Wood (2013), Multimodel seasonal forecasting of global drought onset, *Geophysical Research*
760 *Letters*, *40*(18), 4900-4905.

761 Zhang, Q., Q. Li, V. P. Singh, P. Shi, Q. Huang, and P. Sun (2018), Nonparametric integrated agrometeorological
762 drought monitoring: Model development and application, *Journal of Geophysical Research: Atmospheres*, *123*(1), 73-
763 88.

764

765

766

767

768

769

770